

THE DRAGONFLY NEARBY GALAXIES SURVEY. II. ULTRA DIFFUSE GALAXIES NEAR THE ELLIPTICAL GALAXY NGC 5485

ALLISON MERRITT¹, PIETER VAN DOKKUM¹, SHANY DANIELI^{1,5,6}, ROBERTO ABRAHAM^{2,3}, JIELAI ZHANG^{2,3}, I. D. KARACHENTSEV⁷, L. N. MAKAROVA⁷

Draft version October 7, 2016

ABSTRACT

We present the unexpected discovery of four ultra diffuse galaxies (UDGs) in a group environment. We recently identified seven extremely low surface brightness galaxies in the vicinity of the spiral galaxy M101, using data from the Dragonfly Telephoto Array. The galaxies have effective radii of $10'' - 38''$ and central surface brightnesses of $25.6 - 27.7$ mag arcsec⁻² in g-band. We subsequently obtained follow-up observations with *HST* to constrain the distances to these galaxies. Four remain persistently unresolved even with the spatial resolution of *HST*/ACS, which implies distances of $D > 17.5$ Mpc. We show that the galaxies are most likely associated with a background group at ~ 27 Mpc containing the massive ellipticals NGC 5485 and NGC 5473. At this distance, the galaxies have sizes of $2.6 - 4.9$ kpc, and are classified as UDGs, similar to the populations that have been revealed in clusters such as Coma, Virgo and Fornax, yet even more diffuse. The discovery of four UDGs in a galaxy group demonstrates that the UDG phenomenon is not exclusive to cluster environments. Furthermore, their morphologies seem less regular than those of the cluster populations, which may suggest a different formation mechanism or be indicative of a threshold in surface density below which UDGs are unable to maintain stability.

1. INTRODUCTION

The lowest detectable surface brightnesses of galaxies are, in practical terms, a function of survey depth (Disney 1976; Dalcanton et al. 1995). Low surface brightness galaxies (LSBGs) are known to exist at all sizes (e.g. Zucker et al. 2006; McGaugh & Bothun 1994; Bothun et al. 1987) and across all environments, from the field (Impey et al. 1996) to the Local Group (McConnachie 2012) to massive clusters such as Virgo and Coma (Ulmer et al. 1996; Impey et al. 1988; Caldwell 2006; Adami et al. 2006; Davies et al. 2016). When compared to high surface brightness galaxies (HSBGs) of either similar luminosity or effective radius, the integrated number density of LSBGs surpasses that of HSBGs (Dalcanton et al. 1997). And, as advances in instrumentation (e.g. Abraham & van Dokkum 2014) and methodology allow observations to push down to ever lower surface brightness limits, the diversity of the low surface brightness universe is continuously unveiled.

Recently, a population of ultra diffuse galaxies (UDGs) featuring extremely low central surface brightnesses ($\mu_{g,0} > 24$ mag arcsec⁻²) and large effective radii ($R_e > 1.5$ kpc) was identified in the outskirts of the Coma cluster by van Dokkum et al. (2015); and subsequent searches

in the Virgo (Mihos et al. 2015) and Fornax (Muñoz et al. 2015) clusters revealed similar (though less numerous) populations.

van Dokkum et al. (2016) measured the stellar velocity dispersion of Dragonfly 44 (Coma-DF44, hereafter DF44), one of the largest UDGs in the Coma cluster, and showed that the dark matter fraction within the effective radius is 98%. Similarly, globular cluster counts in two other UDGs – Dragonfly 17 (Coma-DF17, hereafter DF17) in Coma (Peng & Lim 2016; Beasley & Trujillo 2016) and VCC 1287 in Virgo (Beasley et al. 2016) – indicate that these are systems with unusually high total mass-to-light (or total-to-stellar mass) ratios for their masses. While it seems clear that all three of these galaxies are underluminous for their total mass (or globular cluster count), UDGs do *not* all have the same mass. DF44 is likely hosted by a massive ($\sim 10^{12} M_\odot$) dark matter halo, whereas the other two UDG host halos are less massive, with reported estimates between $8 \times 10^{10} M_\odot - 10^{11} M_\odot$ (see van Dokkum et al. 2016).

It is not yet understood how UDGs form, but considering that UDGs are empirically defined solely on the basis of their size and surface brightness, it is reasonable to expect that multiple formation mechanisms may be at play. The UDGs VCC 1287, Dragonfly 44, and Dragonfly 17 seem to be “failed” galaxies that are underluminous for their mass (Beasley & Trujillo 2016; van Dokkum et al. 2016). There could plausibly be additional, fundamentally different systems that fall into the UDG category as well. Amorisco & Loeb (2016) suggest, for example, that dwarf galaxies residing in dark matter halos with high spin have large sizes (and thus low surface brightnesses) and would therefore be observationally classified as UDGs. Any such objects are likely distinct from DF44, DF17 and VCC 1287, however, as all three of these galaxies are large and underluminous relative to their globular cluster systems. Finally, some UDGs could

¹ Department of Astronomy, Yale University, 260 Whitney Avenue, New Haven, CT 06511, USA

² Department of Astronomy and Astrophysics, University of Toronto, 50 St. George Street, Toronto, ON, Canada M5S 3H4

³ Dunlap Institute for Astronomy and Astrophysics, University of Toronto, Toronto ON, M5S 3H4, Canada

⁴ Canadian Institute for Theoretical Astrophysics, Toronto, ON, M5S 3H4, Canada

⁵ Yale Center for Astronomy and Astrophysics, Yale University, New Haven, CT 06520, USA

⁶ Department of Physics, Yale University, New Haven, CT 06520, USA

⁷ Special Astrophysical Observatory, Nizhnij, Arkhyz, Karachai-Cherkessia 369167, Russia

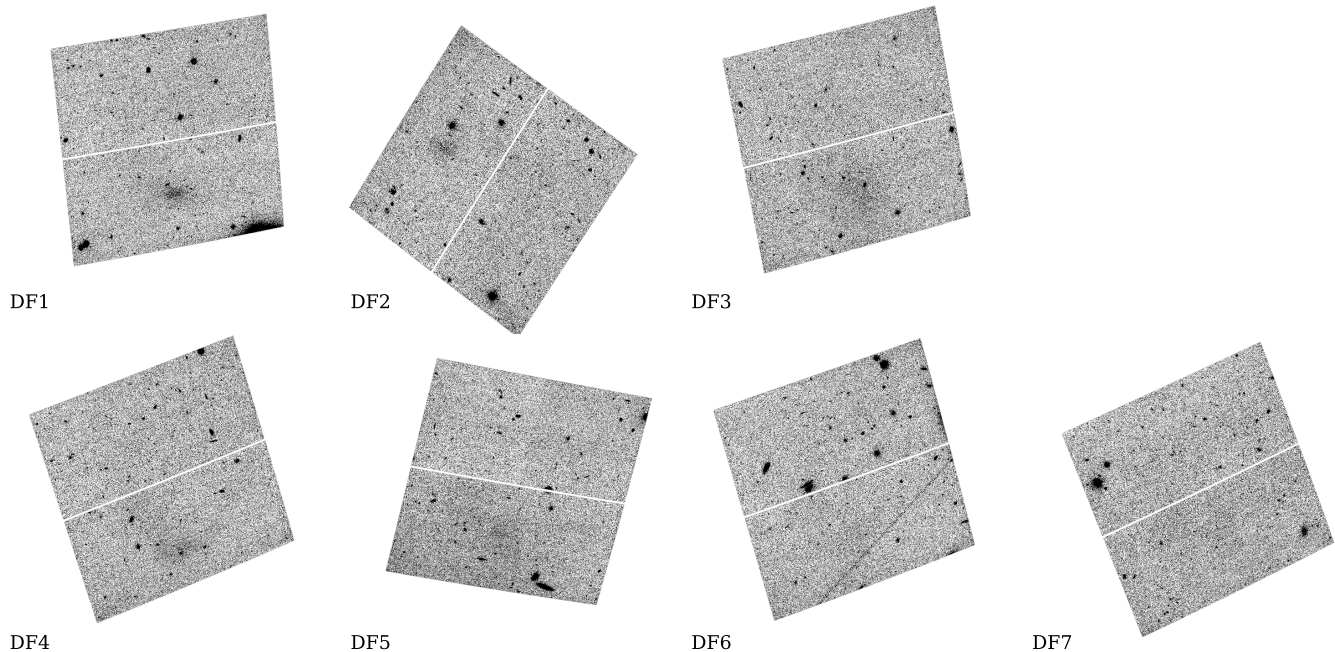


Figure 1. HST images of all seven LSB galaxies reported in Merritt et al. (2014). Observations were obtained in F606W and F814W, with 0.5 orbits each, although here we show only F606W. North is up and East is to the left. The field of view is ~ 3.5 arcminutes on a side.

also be normal dwarfs disrupting in harsh cluster environments (Moore et al. 1996), analogous to disrupting dSphs in the Local Group (e.g. Collins et al. 2013).

In addition to mass measurements, understanding UDGs and their properties as a function of environment is key to determining how and where UDGs form. This is a nontrivial task, however, as the low surface brightness nature of UDGs means that obtaining reliable distance measurements ranges from difficult to nearly impossible. Dalcanton et al. (1997) obtained spectroscopic redshifts of seven field LSBGs, two of which are large enough and faint enough to qualify as UDGs. More recently, Toloba et al. (2016) and Crnojević et al. (2016) measured the distances to relatively nearby (and likely disrupting) UDGs associated with the spiral galaxy NGC 253 and the massive elliptical NGC 5128 (Cen A), respectively, via the Tip of the Red Giant Branch method. Finally, Makarov et al. (2015) and Martínez-Delgado et al. (2016) were able to spectroscopically confirm the presence of UDGs in low density regions.

In this paper, we present evidence for the existence of UDGs in a group environment. We use *HST* observations to constrain the distances to seven previously identified LSBGs (Merritt et al. 2014), and find that four of the seven must lie at distances > 17.5 Mpc. The lower limits on distance translate into minimum sizes, and we classify these galaxies as UDGs. We assess the likely environment of the sample and discuss the implications of a population of group UDGs.

2. IMAGING

2.1. Dragonfly

The diffuse galaxies examined in this work were originally discovered in data taken by the Dragonfly Telescope Array (Abraham & van Dokkum 2014), in a field

centered on the nearby spiral galaxy M101 (Merritt et al. 2014; we note that the galaxies are also visible in images taken on 0.1–0.8 m amateur telescopes by Karachentsev et al. 2015 and Javanmardi et al. 2016). Dragonfly is a robotic, refracting telescope designed specifically for the detection of extended, extremely low surface brightness optical emission.

The raw data frames were taken in the Spring of 2013, for a total of ~ 35 hours. Full details of data collection and the data reduction pipeline are given in van Dokkum et al. (2014) and Merritt et al. (2014). In brief, we obtain calibration frames each night and apply these to the individual frames. We model and correct for a sky gradient produced by changes in the sky background with zenith distance with a second order polynomial after aggressively masking all objects in the frame.

The final reduced images are constructed from *g*-band and *r*-band frames, and have a limiting surface brightness of $\mu_g \sim 29.5$ mag arcsec $^{-2}$ and $\mu_r \sim 29.8$ mag arcsec $^{-2}$ when measured in $10''$ boxes. Star-subtracted images were also required for a robust detection of low surface brightness galaxies (Merritt et al. 2014); these were produced using a custom pipeline that builds and applies an empirical, spatially varying composite PSF (described in detail in Merritt et al. 2016).

2.2. HST

The optical colors, luminosities, and morphologies of the seven LSBGs are consistent with being satellite galaxies associated with M101 itself; and, as described in Merritt et al. (2014), none possess the large-scale wispy structure characteristic of galactic cirrus (e.g. Guhathakurta & Tyson 1989). We cannot derive their distances from Dragonfly photometry alone, however. We therefore obtained follow-up data with *HST*, as the

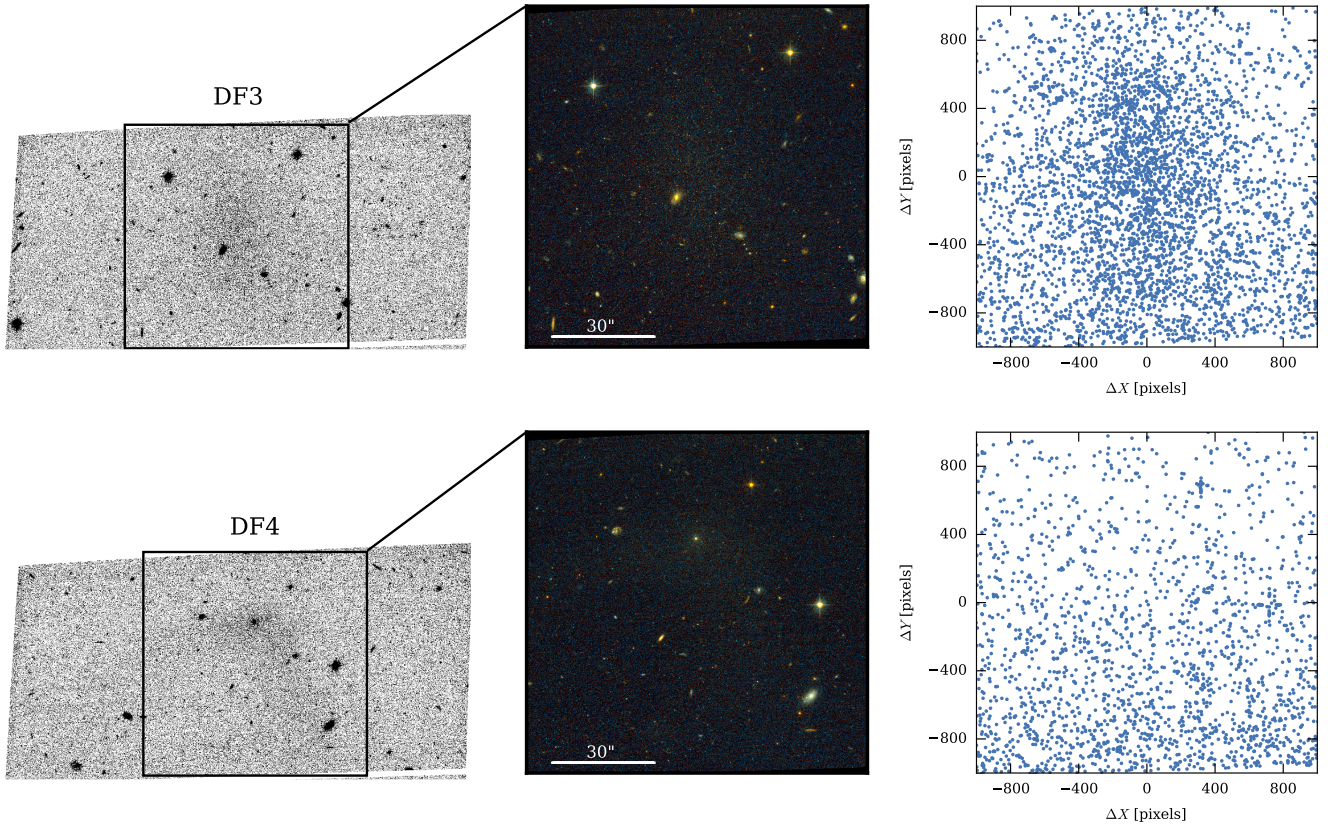


Figure 2. Left: greyscale *HST* images of DF3 and DF4 (*F606W*). These two LSBGs have very similar sizes and central surface brightnesses (see Table 1). Middle: zoomed in color images of DF3 and DF4, created from *F606W* and *F814W* images, show that the galaxies are very different at *HST* resolution – DF3 resolves into a sea of faint stars, whereas DF4 appears to be an empty image. This is demonstrated more clearly in the far right panel, where we show the distribution of point sources in both images as determined by DOLPHOT.

higher spatial resolution ($0.05 \text{ arcsec pixel}^{-1}$) should provide photometry of resolved stars in each of these galaxies if they are in fact members of the M101 group (at a distance modulus of 29.04, or $\sim 6.4 \text{ Mpc}$; Shappee & Stanek 2011).

The *HST* data were obtained through the *HST* program 13682 and consist of ACS/WFC imaging. Each galaxy was observed for 0.5 orbits with both the *F606W* and *F814W* filters. The data were reduced with the default *HST* reduction pipeline, and the drizzled *HST* images (generated with *Astrodizzle* from the individual calibrated images) for the seven galaxies are shown in Figure 1.

We find a remarkable, qualitative difference between the galaxies. Three are resolved into hundreds of stars, as expected for a distance of $\sim 7 \text{ Mpc}$. These three galaxies (DF1, DF2, and DF3 in the Merritt et al. (2014) nomenclature) are described in a companion paper (Danieli et al. 2016, submitted). However, the remaining four (DF4, DF5, DF6 and DF7) are, at first inspection, *undetected* in our *HST* imaging. The differences between the resolved and unresolved galaxies is illustrated in Figure 2. We select DF3 and DF4 as example galaxies, as they have nearly identical central surface brightness and size (Table 1). Despite this, when we examine the images at full *HST* resolution and the associated distributions of point sources detected with DOLPHOT (from Danieli et al.), DF3 emerges as a clear overdensity while DF4

appears to be an empty image. These two galaxies are representative of the differences between the two subsets of galaxies. Only after binning and smoothing can we infer the presence of large, diffuse objects in the images of DF4-DF7 – although DF5-DF7 are better visually described as large scale background variations than obvious objects (see Figure 1).

Figure 3 displays greyscale images of all four unresolved galaxies (as observed with Dragonfly); color images of the central 100 arcsec of each field, created from *HST F606W* and *F814W* data, are shown in Figure 4.

2.3. CFHT

The fact that these four galaxies do not resolve into stars raises the question of whether our detection algorithm picked up noise peaks or artifacts in the Dragonfly data. This is particularly a concern for DF6 and DF7, which are not significantly detected with *HST* even after binning and smoothing.

Fortunately, the M101 field has excellent additional datasets which settle this question. The field has deep, public CFHT imaging obtained in the context of the Canada-France-Hawaii Telescope Lensing Survey (CFHTLS Heymans et al. 2012). We obtained the reduced data from the CFHT archive; the data were processed first with the standard ELIXIR (Magnier & Cuillandre 2004) software and then with the THELI data reduction pipeline (Erben et al. 2005). The exposure times

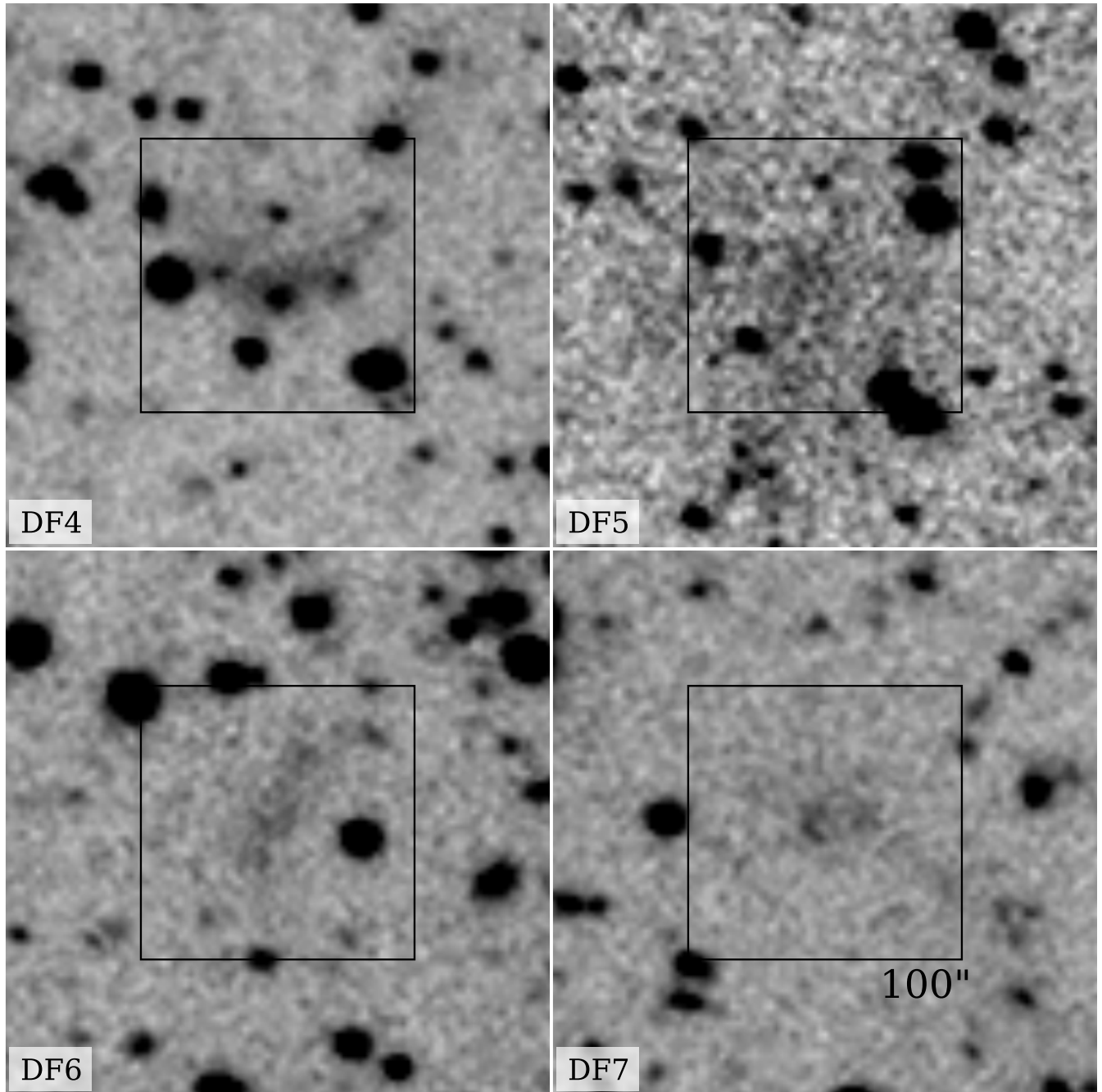


Figure 3. Dragonfly discovery images of the four unresolved LSBGs. The cutouts are 200 arcsec on a side, with black boxes highlighting the central 100 arcsec. The galaxies are all extremely large and diffuse, but beyond that show a high degree of morphological diversity.

were 2500 s per filter.

The CFHT images of the four galaxies are shown in Figure 5. All four objects are clearly detected, and a comparison between Figures 3 and 5 shows that their morphologies are consistent between the two datasets.

Figure 6 demonstrates that the apparent sizes of the galaxies are somewhat dependent on the dataset, however. In particular, DF5 is the largest of the Dragonfly-detected sample, but the smallest of the CFHTLS-detected sample. The low spatial resolution of Dragonfly could, in principle, result in an overestimated size if unresolved background structures are erroneously included

in the light of the galaxy in question. Dragonfly is optimized to detect spatially-extended emission, however, so another possibility is that the CFHTLS data is less sensitive to the extremely diffuse outskirts of the galaxies.

As a test, we bin the CFHT data to match the spatial resolution of Dragonfly (approximately 10×10 pixels) and then median-smooth with a kernel of 3 pixels to enhance the low surface brightness outskirts (Figure 7). The Dragonfly data were also median-smoothed for consistency. After binning and smoothing, DF5 is still smaller in the CFHT image than in the Dragonfly image. However, we can see that this process has indeed

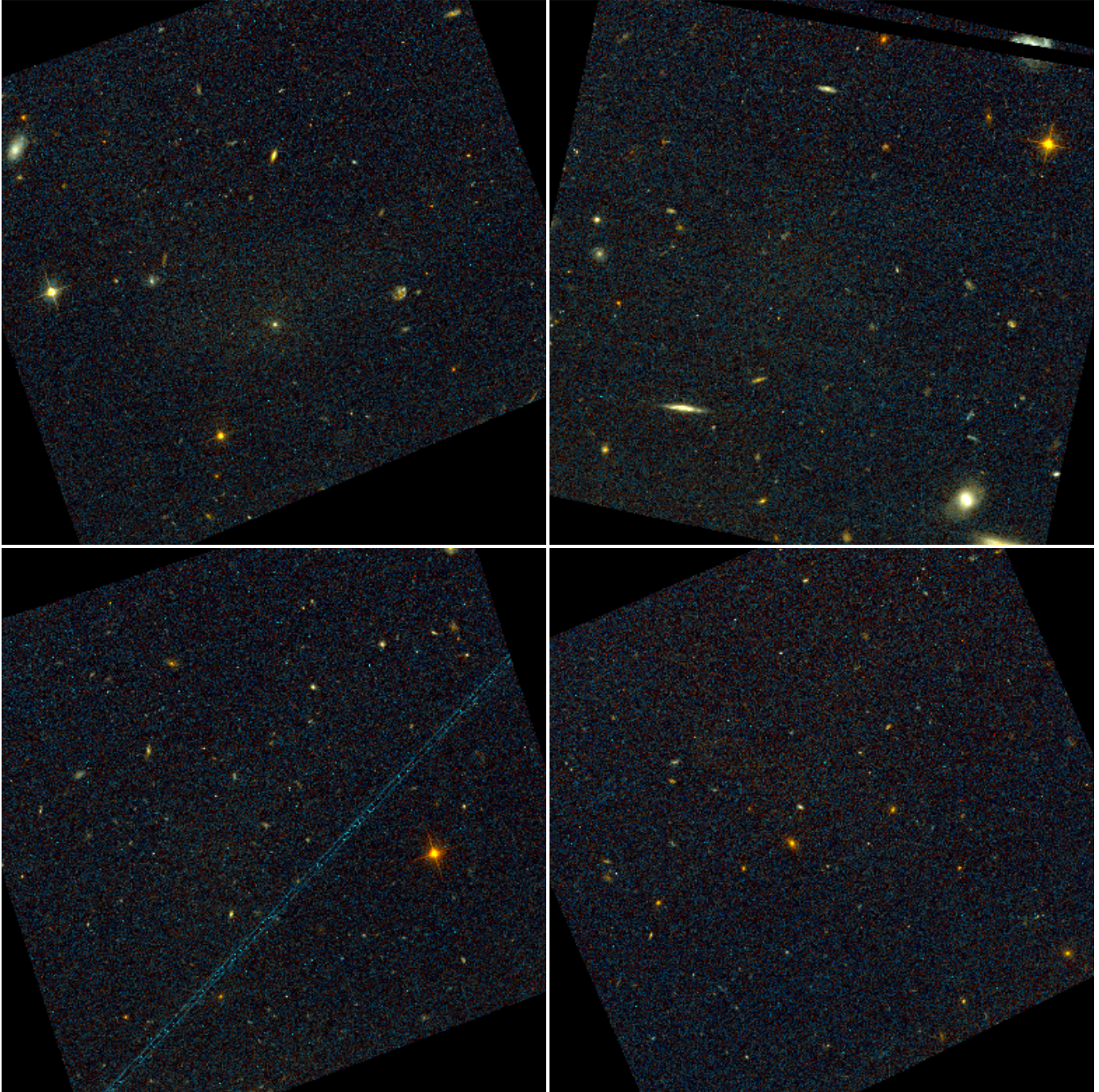


Figure 4. HST pseudo-color images of the galaxies (the area corresponds to the 100 arcsec/side boxed regions in Figure 3), created from the F606W and F814W images. The four unresolved galaxies are barely visible in these data, although they re-emerge in binned data (Figure 6).

increased the flux at large radii, indicating that the most likely culprit is either the surface brightness limits of the CFHT data or possibly an overestimate of the background level during sky subtraction. We therefore adopt the values of surface brightness, structure and sizes measured in the Dragonfly data for the remainder of this paper.

3. DISTANCE MEASUREMENTS

3.1. A lower distance limit based on HST images

For nearby galaxies, the Tip of the Red Giant Branch (TRGB) I -band luminosity provides a reliable distance estimator as it corresponds to a constant value of $M_I^{TRGB} \sim -4$ mag (e.g., Gallart et al. 2005). This technique relies on the ability to detect individual RGB stars, however, and we can therefore use the fact that we are *unable* to resolve these galaxies with *HST* to place lower limits on their distances.

In Danieli et al. (2016, submitted) we use the publicly available DOLPHOT software package (Dolphin 2000) in combination with the TRGBTOOL software (Makarov



Figure 5. CFHT pseudo-color images of the LSBGs (the area corresponds to the 100 arcsec/side boxed regions in Figure 3), created from g and r -band data.

et al. 2006) to determine the limiting magnitude for each resolved LSBG (DF1, DF2, and DF3). In brief, we create an artificial star list based on the photometry of each LSBG, place the stars into the *HST* images, and use the resulting DOLPHOT outputs to measure the completeness as a function of magnitude.

We find that the data reach 50% completeness at $27.2^{+0.04}_{-0.03}$ magnitude in I -band ($F814W$). This value is the average of the results for DF1, DF2, and DF3; the error bars encompass the full variation between the three *HST* fields. To first order, then, we can infer a minimum

distance modulus of 31.2 mag from an undetected TRGB, corresponding to a lower distance limit of 17.5 Mpc. We note that for a galaxy at the distance of M101, we would expect to observe the TRGB at an I -band magnitude of ~ 25 .

3.2. Association with the NGC 5485 group

From the lower bounds on the distances to the galaxies, we infer that they cannot be members of the M101 group, and we turn to the surrounding field for clues of their local environment.

Figure 8 shows the full Dragonfly field centered on

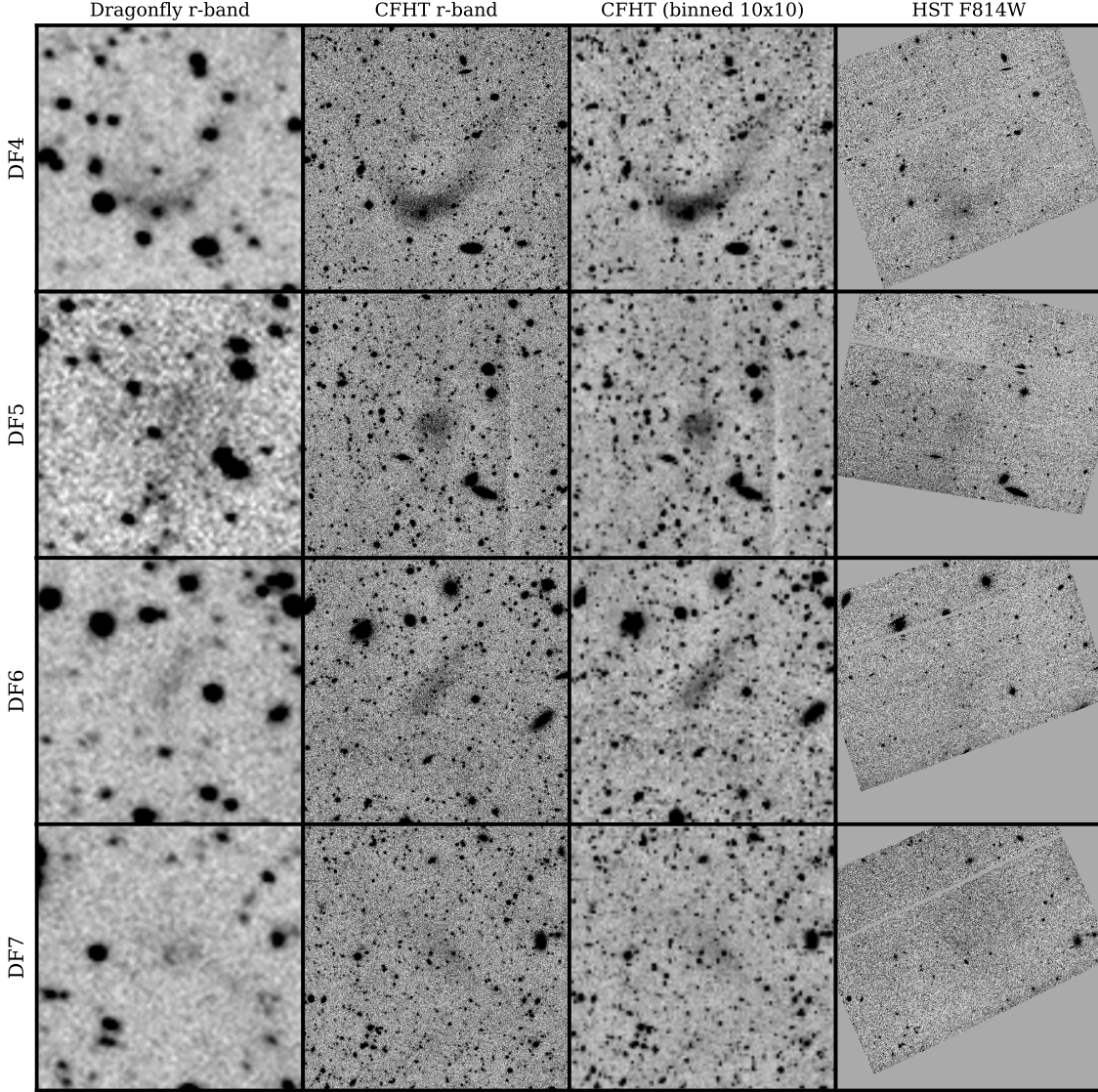


Figure 6. Each row represents an individual LSBG (DF4-DF7). From left to right we show: the Dragonfly r-band cutout, as presented in Merritt et al. (2014); the CFHT r-band cutout; the same CFHT r-band cutout binned to match the spatial resolution of Dragonfly; and the HST F814W cutout. Each box is 200 arcsec on a side. In the Dragonfly images, any overlapping stars were removed prior to analysis.

M101 where these galaxies were discovered. The zoomed panels show CFHT color images of the galaxies and highlight their positions in the field. As previously noted by Merritt et al. (2014), all four lie to the East of M101; they appear to be distributed nearly uniformly around NGC 5485, a massive elliptical galaxy at a distance of ~ 27 Mpc (Tully et al. 2016).

The galaxies appear to be consistent with the projected locations of NGC 5485 and its associated group, which has NGC 5473 as its brightest member Tully (2015). However, the Tully (2015) group catalog is optimized for

$3,000 \lesssim v_r \lesssim 10,000 \text{ km s}^{-1}$ and suffers from uncertainties due to large peculiar velocities for $v_r \lesssim 3,000 \text{ km s}^{-1}$ (the regime relevant for all nearby groups of interest) as well as incompleteness. We therefore supplement it with the Makarov & Karachentsev (2011) groups catalog, which is more accurate for nearby groups (Makarov & Karachentsev 2011; Tully 2015). Figure 9 displays a zoom-in on the members of the NGC 5473 group, with symbol sizes of group members scaled by their absolute B magnitude. The positions of the galaxies, denoted by star symbols, are centered on and distributed throughout

Table 1
Physical Properties of the UDGs

ID	α (J2000)	δ (J2000)	g^a	$\mu_{0,g}^b$	$\mu_{e,g}^c$	$g-r$	r_e^d	r_e^e	n^f	b/a^g
M101-DF4	211.88932	54.710178	18.8 ± 0.3	26.8 ± 0.4	27.9 ± 0.2	0.6 ± 0.4	28 ± 7	3.6 ± 0.9	0.7 ± 0.3	0.6 ± 0.1
M101-DF5	211.11709	55.616788	18.0 ± 0.2	27.4 ± 0.3	28.0 ± 0.2	0.4 ± 0.4	38 ± 7	4.9 ± 0.9	0.4 ± 0.2	0.8 ± 0.1
M101-DF6	212.07927	55.190214	20.1 ± 0.4	27.5 ± 1.1	27.8 ± 0.4	0.4 ± 0.5	22 ± 8	2.9 ± 1.0	0.3 ± 0.8	0.3 ± 0.1
M101-DF7	211.45134	55.132899	20.4 ± 0.6	27.7 ± 1.6	28.7 ± 0.6	0.9 ± 0.8	20 ± 9	2.6 ± 1.1	0.6 ± 1.0	0.5 ± 0.2

Note. — Structural parameters were computed using GALFIT, from a stack of Dragonfly g - and r -band images.

^a Integrated apparent magnitude, calibrated to SDSS.

^b Central surface brightness, in mag arcsec^{-2} .

^c Effective surface brightness, in mag arcsec^{-2} .

^d Effective radius, in arcsec.

^e Effective radius, in kpc, assuming a distance of 27 Mpc.

^f Sersic index.

^g Axis ratio.

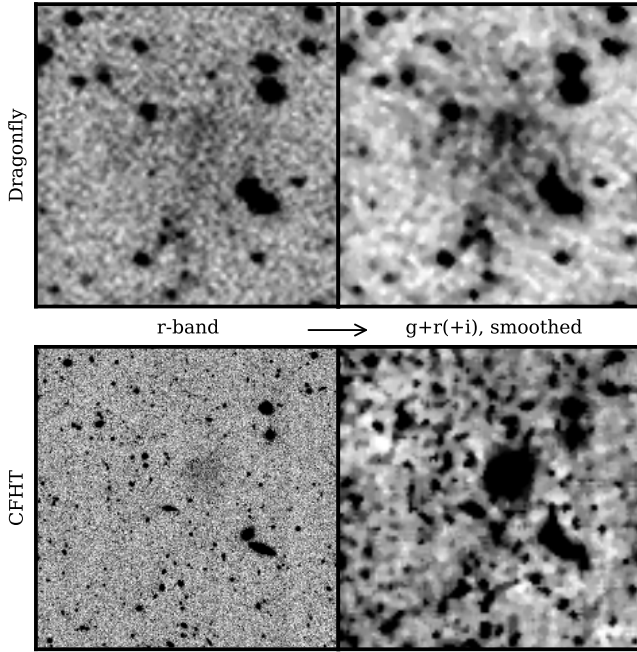


Figure 7. The LSB galaxy DF5 is shown here in Dragonfly and CFHT data. The reduced data are shown in the left column. In the right column, the Dragonfly image has been median-smoothed (3×3 pixels), and the CFHT image has been first binned to match the spatial resolution of Dragonfly and then median-smoothed in the same way. While the size of DF5 is apparently smaller in the CFHT data than in Dragonfly in both cases, in the binned/smoothed image faint emission can be seen extending out much farther than the reduced image reveals. Additionally, CCD defects in the CFHT data can be seen in both images. We therefore use only the Dragonfly data from this point onward.

the group.

4. RESULTS

4.1. Sizes

Given their projected proximity to the NGC 5485 group, we adopt a distance of 27 Mpc for the four unresolved LSBGs. At this distance, their physical sizes range from 2.6 ± 1.1 to 4.9 ± 0.9 kpc.

These sizes, in combination with the low central surface brightnesses, are large enough to allow us to classify the unresolved LSBGs as UDGs, a population of galaxies

empirically defined by [van Dokkum et al. \(2015\)](#) to have extremely low central surface brightness ($\mu_{g,0} > 24 \text{ mag arcsec}^{-2}$) and large sizes ($R_e > 1.5 \text{ kpc}$).

We provide a graphical summary of known (available) low surface brightness galaxy catalogs in Figure 10. We note that classically, LSBGs are defined on the basis of the central surface brightness of the disk, irrespective of the presence of a bulge component. In order to provide the most fair comparison with our sample, we consider only bulgeless LSBGs with $n \leq 1$. The zoom box highlights the empirically defined UDG region ($\mu_{0,g} > 24 \text{ mag arcsec}^{-2}$ and $R_e > 1.5 \text{ kpc}$). The galaxies presented here (shown in Figure 10 as large green symbols) are a sample of UDGs observed in a group environment, and are among the most extreme objects of their class in terms of surface brightness.

4.2. Colors and morphologies

The morphologies of these four UDGs are highly nonuniform, with axis ratios ($0.3 \leq b/a \leq 0.9$). The colors and structural parameters as measured from Dragonfly photometry were reported in [Merritt et al. \(2014\)](#), and we summarize these along with the physical sizes of each galaxy in Table 1. The average $g-r$ color of the sample is $\langle g-r \rangle = 0.57$, similar to the average color of the low luminosity end of the sample studied by [van der Burg et al. \(2016\)](#).

The group UDGs display a noteworthy degree of morphological diversity when compared to the cluster UDGs. The latter are predominantly round (e.g. [van Dokkum et al. 2015](#); [Mihos et al. 2015](#)), whereas the galaxies presented here have a large range of ellipticities (see Table 1). One galaxy (DF4) has a boomerang-like shape, and is possibly undergoing tidal stripping. The largest, DF5, is the roundest of the sample; the remaining two (DF6 and DF7) are elongated. Despite these differences, however, the surface brightness profiles of group and cluster UDGs alike fall off exponentially, occasionally featuring a central depression (that is, $n < 1$, as measured by [Merritt et al. 2014](#); [van Dokkum et al. 2015](#), see also Table 1).

There are no apparent trends between color and morphology in this small sample.

5. DISCUSSION

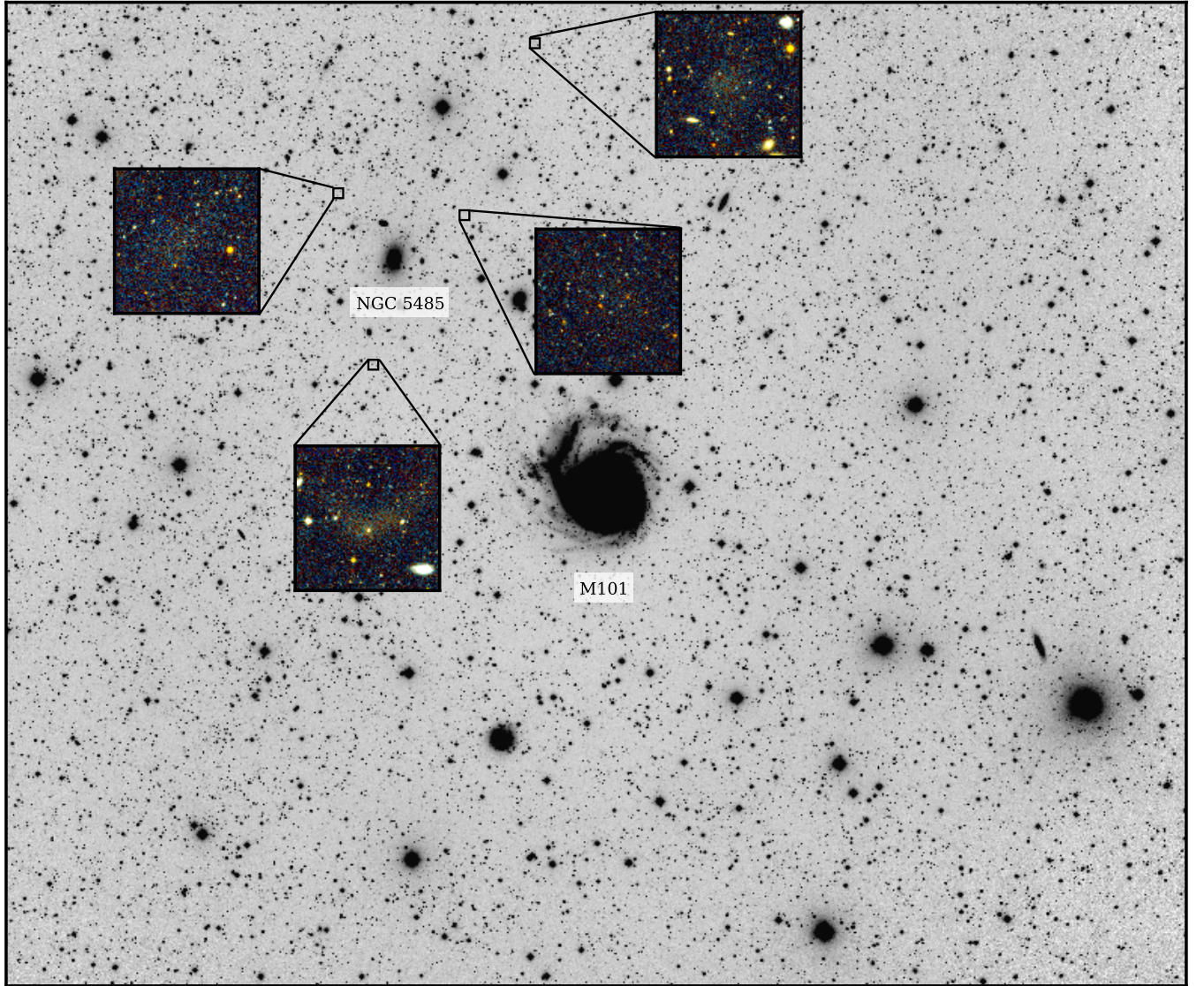


Figure 8. The Dragonfly field of view is shown in greyscale, with zoom insets showing the locations of the four LSBGs. The color images were created using CFHT g- and r-band data.

5.1. UDGs outside of the cluster environment

The minimum distance to the four unresolved LSBGs places strong lower limits on their sizes and confirms their status as UDGs; the projected spatial distribution of the galaxies strongly suggests that they are members of the NGC 5473 group at a distance of ~ 27 Mpc, providing further evidence that UDGs are not a phenomenon that is exclusive to cluster environments.

Thus far, the growing observational census for the UDG population suggests that UDGs are preferentially associated with massive early-type galaxies, with the

presence of cluster UDGs in particular becoming increasingly well documented (Impey et al. 1988; O’Neil et al. 1997a; Bothun et al. 1991; Ulmer et al. 1996; Caldwell 2006; van Dokkum et al. 2015; Davies et al. 2016; Mihos et al. 2015; Koda et al. 2015; Muñoz et al. 2015; van der Burg et al. 2016; Yagi et al. 2016). Additional evidence in support of this picture comes from Muñoz et al. (2015), who found that the non-nucleated LSBG population in Fornax has a projected spatial distribution that clusters around the locations of giant ellipticals (we note however, that their sample contains very few UDGs); from van der Burg et al. (2016), who showed that the number density

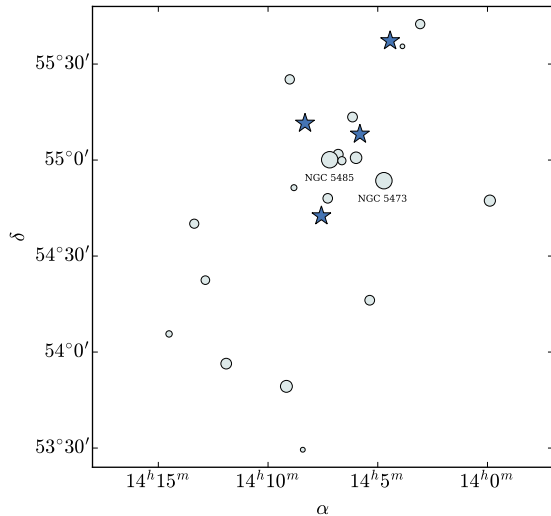


Figure 9. The members of the NGC 5485 group (Makarov & Karachentsev 2011), with symbol sizes scaled by absolute B magnitude (Makarov et al. 2014). The locations of the four LSBGs are shown as well (blue stars; no luminosity scaling); the projected positions are consistent with group membership.

of UDGs in clusters is correlated with cluster halo mass; and from Roman & Trujillo (2016) who reported that UDGs tend to be located within large-scale structures.

Examples of UDGs with either established (Makarov et al. 2015; Martínez-Delgado et al. 2016) or implied (Dalcanton et al. 1997; O’Neil et al. 1997a) lower density environments do exist, however. And, recently, they have even been associated with spiral galaxies – specifically in the cases of And XIX in the Local Group (McConnachie 2012) and Scl-MM-Dw2 in the NGC 253 group (Toloba et al. 2016).

To quantify the population of UDGs in group environments, we compare the number of known UDGs to the number of bright ($M_B < -17$) group members. We obtain group membership information from Makarov & Karachentsev (2011), and absolute B -band magnitudes from Makarov et al. (2014). The 4 UDGs presented here, relative to the 6 bright members of the NGC 5473 group, constitute a relatively rich UDG population when compared to the Local Group (1 known UDG per 6 bright members). The NGC 253 and Cen A groups each have 1 known UDG as well, compared to 2 and 4 bright members, respectively. Although it is unclear based on this small sample whether we should necessarily expect a tight correlation between the number of bright members and the number of UDGs in a given environment, these numbers do suggest that there should be at least one observable UDG per nearby group.

5.2. Structural stability

Key questions regarding the UDG population include: Is this a stable population, or are we witnessing their disruption and the subsequent buildup of intragroup and intracluster light? If they are stable, how can such diffuse galaxies survive?

The three cluster UDGs – DF44, DF17 and VCC 1287 – that have been studied in detail thus far have all been

shown to have very high mass-to-light ratios in their central regions (van Dokkum et al. 2016; Beasley et al. 2016; Beasley & Trujillo 2016). All three have globular cluster systems (and, in the case of DF44, a stellar velocity dispersion) that are typical of galaxies in relatively massive dark matter halos, and a stellar component that is significantly underluminous. In combination with their (undisturbed) spheroidal morphologies and old stellar populations, these galaxies can potentially be thought of as “failed” L_* or dwarf galaxies that lost their gas early on (e.g., by ram pressure stripping, Gunn & Gott 1972).

An alternate explanation is that some UDGs are either the descendants of classical (bulgeless) LSBGs, which are thought to reside in massive, low density dark matter halos (e.g. Dalcanton et al. 1995; de Blok & McGaugh 1996); or, possibly, “almost-dark” (e.g. Cannon et al. 2015) that fell into denser environments. In this scenario, the colors and morphologies of the otherwise slowly-evolving LSBGs (van den Hoek et al. 2000) could be explained by an accelerated evolution induced by interactions with neighbors in high density environments (O’Neil et al. 1997b). Gnedin (2003) showed that although the most diffuse and extended LSBGs are fated to disrupt in cluster environments (see also Moore et al. 1999), others will simply lose the majority of their halo mass (and up to $\sim 20\%$ of their stellar mass) and transform into spheroidal systems with low central surface densities and large effective radii. This particular scenario is ruled out for DF44, DF17 and VCC 1287, as LSBGs have been shown to contain “normal” globular cluster populations when compared to HSBGs at similar luminosity (Villegas et al. 2008) and if the galaxy had lost (and redistributed) enough mass to transform into a spheroidal UDG, it should have also lost a substantial fraction of its globular clusters. It could, however, potentially explain UDGs with depleted globular cluster systems.

It is worth noting that the Local Group analog of the group and cluster UDGs is And XIX (McConnachie et al. 2008; McConnachie 2012), a dwarf satellite of M31 that is known to be disrupting (Collins et al. 2013). The UDGs recently identified around Cen A and NGC 253 by Crnojević et al. (2016) and Toloba et al. (2016) show evidence for disruption as well, in the form of extended, prominent tidal tails and an elongation towards the central massive galaxy, respectively. Mihos et al. (2015) also reported that one of the three UDGs that they identified in the Virgo cluster (VLSB-A) is disrupting, as indicated by its elongated structure. Additionally, the apparent absence of UDGs in the central regions of the Coma cluster van Dokkum et al. (2015) could be straightforwardly explained if UDGs were unable to survive at small cluster-centric distances; and van der Burg et al. (2016) find that the radial number density distribution of UDGs in eight clusters is consistent with a lack of UDGs within 300 kpc of the cluster centers. It is also worth pointing out that NGC 5485 itself is enveloped by several tidal features (e.g., Karachentsev et al. 2015).

If the four group UDGs presented here are unstable and tidally disrupting, then we should expect to see this reflected in their morphologies. As discussed in Section 4.2, DF4 is highly distorted, with a boomerang-like appearance. DF6 and DF7 are elongated, although not obviously pointed towards the group center (this is not

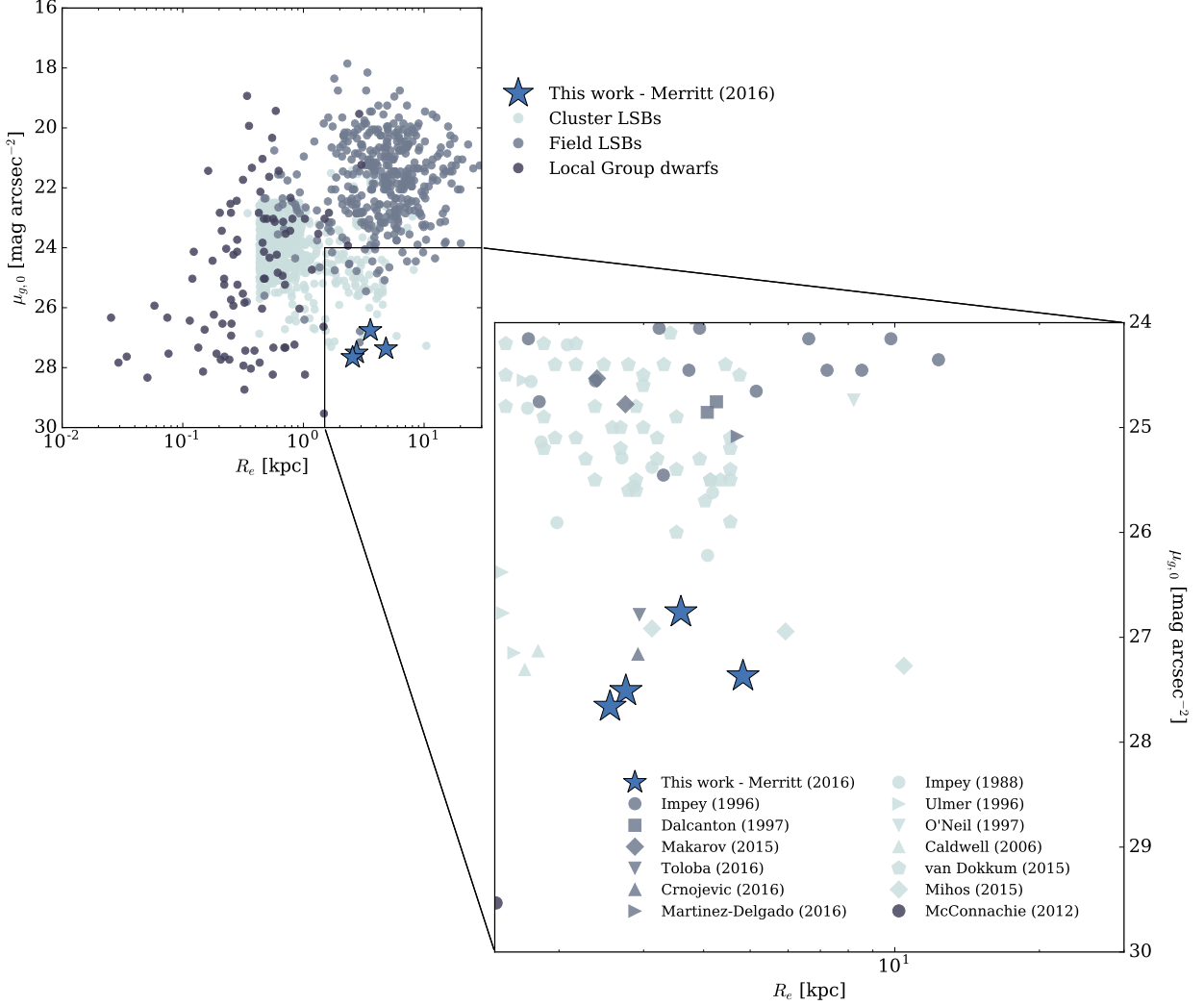


Figure 10. The four group UDGs in the context of other known LSBGs. Upper left: the surface brightness - effective radius plane for LSBs identified in clusters, in the field, and in the Local Group. Lower right: a zoom-in on the region empirically defined to host UDGs. The majority of objects here are found in clusters, although a few are found in lower density environments and one (And XIX) exists in the Local Group. Where necessary, we have converted reported parameters to a cosmology with $H_0 = 70 \text{ km s}^{-1} \text{ Mpc}^{-1}$, and converted from scale length to effective radii. Any required color transformations were done using equations from Blanton & Roweis (2007) and Fukugita et al. (1996). If a study listed an assumed (rather than measured) distance, we assumed the same. We note that a handful of studies shown in the upper left plot do not contain any candidate UDGs – these include Bothun et al. (1991), McGaugh & Bothun (1994), de Blok et al. (1995) and Davies et al. (2016).

ruled out, however, considering projection effects). This would appear to be at odds with the round morphologies and apparently regular appearance of cluster UDGs (the average axis ratio for the Coma sample is 0.7; van Dokkum et al. 2015). A detailed analysis morphologies of cluster UDGs is beyond the scope of this work, but we are investigating this in a separate paper (Mowla et al., in preparation).

In Figure 11, we show the size, axis ratio, and central surface brightness of every known UDG reported here as well as in the literature. Unlike Figure 10, this time we show *only* those UDGs with measured distances (or upper limits); that is, if the discovery paper assumed a distance or association with a background object, we do not include those data points. The UDGs in this work and in the literature are represented by stars and circles,

respectively, and symbols with black borders highlight the UDGs that have been reported to be disrupting. We note that there is an apparent clustering of the disrupting UDGs seen in the lower left panel (in the axis ratio – surface brightness plane), such that they tend to inhabit the lowest surface brightness regime ($\mu_{g,0} > 26.5 \text{ mag arcsec}^{-2}$) and, while they cover a wide range in axis ratios, the majority have $b/a \lesssim 0.7$.

Intriguingly, the roundest UDG in our small sample – DF5 – also has the largest projected distance from the group center (see Figures 8 and 9). If DF5 is *not* associated with the NGC 5485 group, it could be an example of an isolated UDG. The identification of a population of field UDGs would provide critical clues to their formation.

Regardless of whether UDGs are stable or on the brink

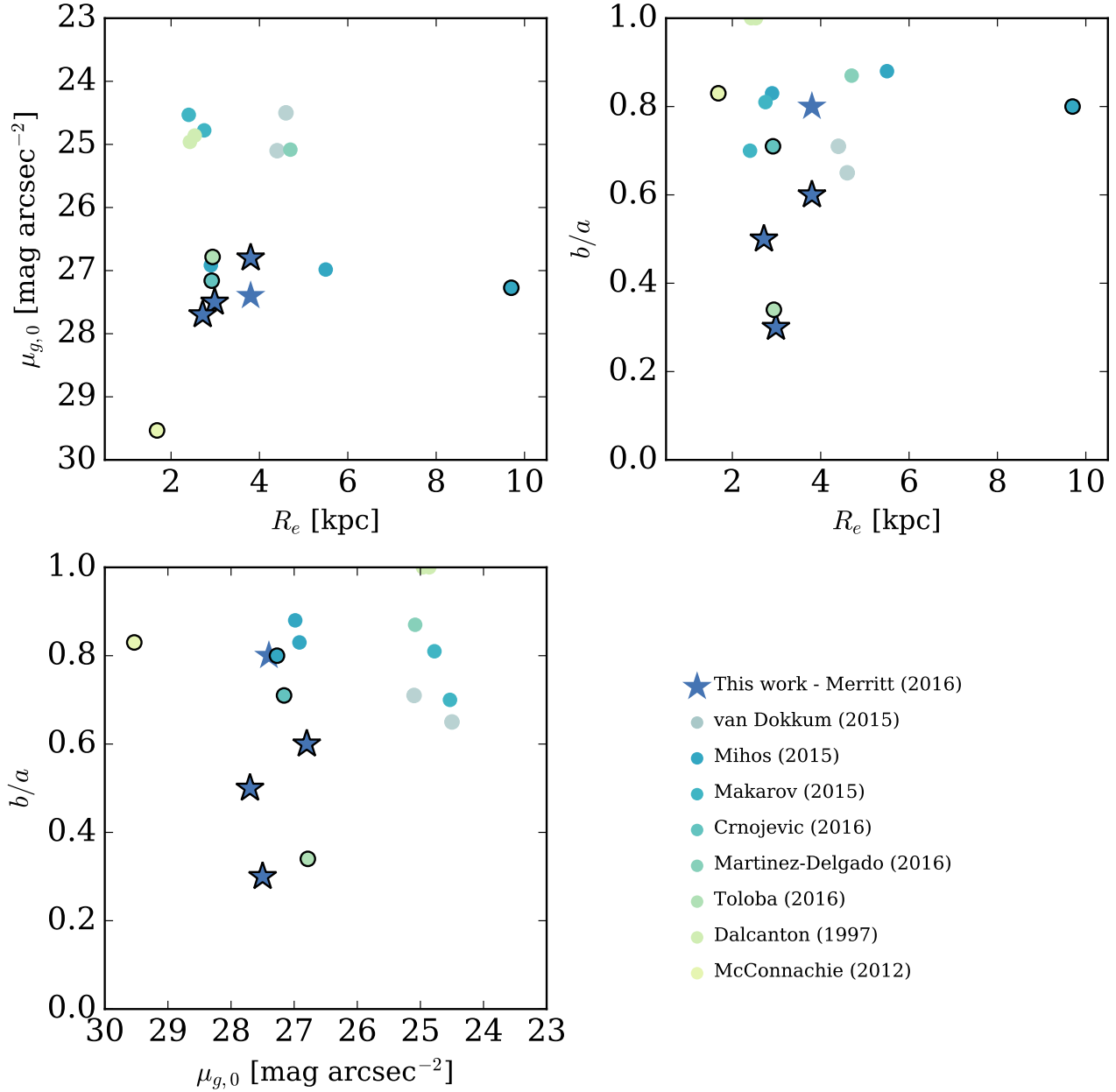


Figure 11. A comparison between the central surface brightnesses, sizes, and axis ratios of known UDGs *with measured distances* (or upper limits on distance). Literature points with black circles indicate cases where the authors describe the galaxy as plausibly disrupting. In general, quoted surface brightnesses in the literature were in V -band; we used reported $B - V$ colors to convert to g -band where possible, and the average of reported colors ($\langle B - V \rangle = 0.72$) otherwise (necessary for data points from Toloba et al. (2016), Martinez-Delgado et al. (2016), and VLSB-C from Mihos et al. (2015)). An exceptions to this, however, is the sample McConnachie (2012), for which we use $\langle B - V \rangle = 0.63$ (the mean color of the brighter Local Group dwarfs, as measured by Mateo 1998). The axis ratio for VLSB-A (from Mihos et al. 2015) is an upper limit.

of disruption, the fact that we observe these galaxies residing in groups suggests that group pre-processing may play a significant role in their formation and subsequent arrival in clusters (Wetzel et al. 2015; Vijayaraghavan & Ricker 2013); in this case we expect that future searches of nearby groups will turn up comparable populations of UDGs.

6. CONCLUSIONS

We have presented follow-up *HST*/ACS observations of four LSBGs discovered in Merritt et al. (2014); the other three resolved galaxies are presented in Danieli et al. (2016, submitted). We placed lower distance limits of 17.5 Mpc based on the lack of resolved stars in the *HST* imaging. Given that the distance to the UDGs

rules out the possibility of a M101 group membership, we consider that they are instead part of the background NGC 5473 / 5485 group, located at ~ 27 Mpc. The projected positions of the UDGs are distributed evenly around the center of the group, consistent with this picture. At this distance, the galaxies have effective radii of $2.6 - 4.9$ kpc, and the large physical sizes combined with the low central surface brightnesses ($\mu_{g,0} = 25.6 - 27.7$ mag arcsec $^{-2}$) qualifies them as UDGs.

Moving forward, it will be critical to expand the census of known UDGs even further, particular to lower density environments. The identification of group UDGs is perhaps not surprising given their apparent ubiquity in clusters, although finding four in a single group is remarkable given that there are only three (with measured distances) known in the Virgo cluster thus far. The morphologies of the group UDGs are, on average, more complex than the morphologies of cluster UDGs. If a significant fraction of the UDG population is comprised of puffed-up dwarfs, then it is possible that we are witnessing that transformation happening.

We thank the anonymous referee for helpful comments that improved the paper. Support from NSERC, NSF grant AST-1312376, grant HST-GO-13682, and from the Dunlap Institute (funded by the David Dunlap Family) is gratefully acknowledged. All authors thank the staff at New Mexico Skies Observatory for their support and assistance; IDK and LNM acknowledge the support of the Russian Science Foundation grant 14-12-00965. AM thanks the BS group for useful discussions.

REFERENCES

- Abraham, R. G., & van Dokkum, P. G. 2014, *PASP*, 126, 55
- Adami, C., Scheidegger, R., Ulmer, M., et al. 2006, *A&A*, 459, 679
- Amorisco, N. C., & Loeb, A. 2016, *MNRAS*, 459, L51
- Beasley, M. A., Romanowsky, A. J., Pota, V., et al. 2016, *ApJ*, 819, L20
- Beasley, M. A., & Trujillo, I. 2016, *ArXiv:1604.08024*
- Blanton, M. R., & Roweis, S. 2007, *AJ*, 133, 734
- Bothun, G. D., Impey, C. D., & Malin, D. F. 1991, *ApJ*, 376, 404
- Bothun, G. D., Impey, C. D., Malin, D. F., & Mould, J. R. 1987, *AJ*, 94, 23
- Caldwell, N. 2006, *ApJ*, 651, 822
- Cannon, J. M., Martinkus, C. P., Leisman, L., et al. 2015, *AJ*, 149, 72
- Collins, M. L. M., Chapman, S. C., Rich, R. M., et al. 2013, *ApJ*, 768, 172
- Crnojević, D., Sand, D. J., Spekkens, K., et al. 2016, *ApJ*, 823, 19
- Dalcanton, J. J., Spergel, D. N., Gunn, J. E., Schmidt, M., & Schneider, D. P. 1997, *AJ*, 114, 635
- Dalcanton, J. J., Spergel, D. N., & Summers, F. 1995, *ArXiv Astrophysics e-prints*
- Danieli, S., van Dokkum, P. G., Merritt, A., Abraham, R. G., Zhang, J., Karachentsev, I. D., & Makarova, L. N. 2016, submitted
- Davies, J. I., Davies, L. J. M., & Keenan, O. C. 2016, *MNRAS*, 456, 1607
- de Blok, W. J. G., & McGaugh, S. S. 1996, *ApJ*, 469, L89
- de Blok, W. J. G., van der Hulst, J. M., & Bothun, G. D. 1995, *MNRAS*, 274, 235
- Disney, M. J. 1976, *Nature*, 263, 573
- Dolphin, A. E. 2000, *PASP*, 112, 1383
- Erben, T., Schirmer, M., Dietrich, J. P., et al. 2005, *Astronomische Nachrichten*, 326, 432
- Fukugita, M., Ichikawa, T., Gunn, J. E., et al. 1996, *AJ*, 111, 1748
- Gallart, C., Zoccali, M., & Aparicio, A. 2005, *ARA&A*, 43, 387
- Gnedin, O. Y. 2003, *ApJ*, 589, 752
- Guhathakurta, P., & Tyson, J. A. 1989, *ApJ*, 346, 773
- Gunn, J. E., & Gott, III, J. R. 1972, *ApJ*, 176, 1
- Heymans, C., Van Waerbeke, L., Miller, L., et al. 2012, *MNRAS*, 427, 146
- Impey, C., Bothun, G., & Malin, D. 1988, *ApJ*, 330, 634
- Impey, C. D., Sprayberry, D., Irwin, M. J., & Bothun, G. D. 1996, *ApJS*, 105, 209
- Javanmardi, B., Martinez-Delgado, D., Kroupa, P., et al. 2016, *A&A*, 588, A89
- Karachentsev, I. D., Riepe, P., Zilch, T., et al. 2015, *Astrophysical Bulletin*, 70, 379
- Koda, J., Yagi, M., Yamanoi, H., & Komiyama, Y. 2015, *ApJ*, 807, L2
- Magnier, E. A., & Cuillandre, J.-C. 2004, *PASP*, 116, 449
- Makarov, D., & Karachentsev, I. 2011, *MNRAS*, 412, 2498
- Makarov, D., Makarova, L., Rizzi, L., et al. 2006, *AJ*, 132, 2729
- Makarov, D., Prugniel, P., Terekhova, N., Courtois, H., & Vauglin, I. 2014, *A&A*, 570, A13
- Makarov, D. I., Sharina, M. E., Karachentseva, V. E., & Karachentsev, I. D. 2015, *A&A*, 581, A82
- Martínez-Delgado, D., Läsker, R., Sharina, M., et al. 2016, *AJ*, 151, 96
- Mateo, M. L. 1998, *ARA&A*, 36, 435
- McConnachie, A. W. 2012, *AJ*, 144, 4
- McConnachie, A. W., Huxor, A., Martin, N. F., et al. 2008, *ApJ*, 688, 1009
- McGaugh, S. S., & Bothun, G. D. 1994, *AJ*, 107, 530
- Merritt, A., van Dokkum, P., & Abraham, R. 2014, *ApJ*, 787, L37
- Merritt, A., van Dokkum, P., Abraham, R., & Zhang, J. 2016, *ArXiv:1606.08847*
- Mihos, J. C., Durrell, P. R., Ferrarese, L., et al. 2015, *ApJ*, 809, L21
- Moore, B., Katz, N., Lake, G., Dressler, A., & Oemler, A. 1996, *Nature*, 379, 613
- Moore, B., Lake, G., Stadel, J., & Quinn, T. 1999, in *Astronomical Society of the Pacific Conference Series*, Vol. 170, *The Low Surface Brightness Universe*, ed. J. I. Davies, C. Impey, & S. Phillips, 229
- Muñoz, R. P., Eigenthaler, P., Puzia, T. H., et al. 2015, *ApJ*, 813, L15
- O’Neil, K., Bothun, G. D., & Cornell, M. E. 1997a, *AJ*, 113, 1212
- O’Neil, K., Bothun, G. D., Schombert, J., Cornell, M. E., & Impey, C. D. 1997b, *AJ*, 114, 2448
- Peng, E. W., & Lim, S. 2016, *ApJ*, 822, L31
- Roman, J., & Trujillo, I. 2016, *ArXiv:1603.03494*
- Shappee, B. J., & Stanek, K. Z. 2011, *The Astrophysical Journal*, 733, 124
- Toloba, E., Sand, D. J., Spekkens, K., et al. 2016, *ApJ*, 816, L5
- Tully, R. B. 2015, *AJ*, 149, 171
- Tully, R. B., Courtois, H. M., & Sorce, J. G. 2016, *AJ*, 152, 50
- Ulmer, M. P., Bernstein, G. M., Martin, D. R., et al. 1996, *AJ*, 112, 2517
- van den Hoek, L. B., de Blok, W. J. G., van der Hulst, J. M., & de Jong, T. 2000, *A&A*, 357, 397
- van der Burg, R. F. J., Muzzin, A., & Hoekstra, H. 2016, *A&A*, 590, A20
- van Dokkum, P., Abraham, R., Brodie, J., et al. 2016, *ApJ*, 828, L6
- van Dokkum, P. G., Abraham, R., & Merritt, A. 2014, *ApJ*, 782, L24
- van Dokkum, P. G., Abraham, R., Merritt, A., et al. 2015, *ApJ*, 798, L45
- Vijayaraghavan, R., & Ricker, P. M. 2013, *MNRAS*, 435, 2713
- Villegas, D., Kissler-Patig, M., Jordán, A., Goudfrooij, P., & Zwaan, M. 2008, *AJ*, 135, 467
- Wetzel, A. R., Deason, A. J., & Garrison-Kimmel, S. 2015, *ApJ*, 807, 49
- Yagi, M., Koda, J., Komiyama, Y., & Yamanoi, H. 2016, *ApJS*, 225, 11
- Zucker, D. B., Belokurov, V., Evans, N. W., et al. 2006, *ApJ*, 650, L41